# Rock Mechanical Investigations and Dimensioning for the new *AkzoNobel* NaCl-Brine Production Field Haaksbergen

Institut
für
Gebirgsmechanik
GmbH

# Rock Mechanical Investigations and Dimensioning for the new *AkzoNobel* NaCl-Brine Production Field Haaksbergen

| | |
|---|---|
| Contractor: | DEEP. Underground Engineering GmbH, Bad Zwischenahn |
| Purchase Order No. (DEEP.): | 22085 (Project 5304-880195) |
| Order No. (IfG): | B IfG 39/2009 |
| Authors: | 5.1.2.e [redacted] |

Leipzig, June 30, 2010

5.1.2.e [redacted]

5.1.2.e [redacted]
Managing Director

**Contents**

# 1. Introduction

A sustainable development of the current brine field in Hengelo is not possible for the long-term (50 years) because the geological and technical possibilities for expansion within the current mining licenses are limited. To ensure the future of the salt industry in Twente the development of a new cavern field is necessary.
To this end Akzo Nobel investigated some areas in the vicinity of Twente concerning the installation of a new NaCl-brine production cavern field resulting in the favoritism of the Haaksbergen area.
Hence Akzo Nobel commissioned an extensive investigation programme for the preferred area Haaksbergen with the following scopes:

- Geology and mining
- Geomechanics
- Leaching concept and brine production, drilling program, well design and borehole completion.

According Phase 1 of the scope, the IfG Institut für Gebirgsmechanik GmbH Leipzig (subcontractor) was commissioned by DEEP Underground Engineering GmbH with the first dimensioning of a new brine production cavern for the Haaksbergen area and with the development of a generic rock mechanical model to demonstrate the capability of the respective cavern field layout.

# 2. Basics of the rock mechanical calculations

## 2.1 Characterization of the calculation program used

The rock mechanical studies carried out base on a numeric model. The rock mechanical model which will be developed in the following has the character of a functional model. That means, it simplifies the actual situation of the deposit as well as the mining situation in a permissible manner.

The calculation program FLAC (ITASCA, 2005[1]) as used for the rock mechanical modelling has been developed particularly for solving geotechnical problems. On an international level, there exists a lot of practical experience in modelling of various rock mechanical problems which has been gained during the last decades. By implementing assumptions with respect to specific material behaviour this calculation program has been further developed and adapted to practical needs.

The calculation code FLAC (Fast Lagrangian Analysis of Continua) utilizes the finite difference method. There, the structure (i.e. the deposit sector as a model body) which has to be investigated is subdivided into a huge number of elements with respective node points. Owing to its discretely pre-determined material behaviour each of these elements responses to the active forces and marginal conditions in a linear or non-linear and rheonomical manner. When the equilibrium conditions are distorted the system begins to oscillate and approaches an equilibrium state according to the given physical opportunities. For each element in correspondence with its adjacent elements this equilibrium state is calculated by solving the complete dynamic equations of motion by means of the explicit LAGRANGE algorithm. Within the used code the effects of large deformations (finite deformations) have been appropriately considered that includes specifically such deformations which play a decisive roll particularly in connection with the creep behaviour of rock salt. These individual elements are characterized by the fact that different properties and parameters such as depth-depending rock pressure, temperature-depending creep rate etc. may be attributed to them in a manner independently from each other.

A specific programming language (FISH) has been implemented into the program code. By means of this language necessary user defined modifications of the implemented material assumptions and/or program flows as well as a specific evaluation of calculated rock mechanical values (state assessment) can be realized.

## 2.2 Visco-elasto-plastic softening model for rock salt

To describe the softening, dilation and creep behavior of salt rocks a visco-elasto-plastic constitutive model has been developed, which is based on a modified MOHR-COULOMB model coupled with a non-linear BURGERS creep model.

[1] ITASCA (2005): Fast Lagrangian Analysis of Continua, Version 5.00, ITASCA Consulting Group Inc. Minneapolis, Minnesota USA

A constitutive model for the description of the softening and dilation behavior of salt rocks should have the following characteristics:

- non-linear failure envelope depending on the minimum principle stress,
- deformation- and stress-dependent softening,
- dominant plastic flow without softening under high confinement,
- dilation depending strongly on the confinement.

On the basis of a modification of the MOHR-COULOMB model, a failure criterion which satisfies the above mentioned demands was developed by MINKLEY (MINKLEY, 2004[2]; MINKLEY et al., 2007[3]):

$$\sigma_{1B} = \sigma_D + N_\phi \cdot \sigma_3 \qquad (2.1)$$

with the function for friction:

$$N_\phi = 1 + \frac{\sigma_{MAX} - \sigma_D}{\sigma_\phi + \sigma_3}. \qquad (2.2)$$

respectively,

$$\sigma_{eff,B} = \sigma_D + \frac{\sigma_{MAX} - \sigma_D}{\sigma_\phi + \sigma_3} \cdot \sigma_3 \qquad (2.3)$$

where $\sigma_3$ = minimum principal stress,

$\sigma_{1B}$ = maximum principal stress at failure,

$\sigma_{eff,B} = \sigma_{1B} - \sigma_3$ = maximum effective stress at failure,

$\sigma_D(\varepsilon^P)$ = uniaxial compressive strength,

$\sigma_{MAX}(\varepsilon^P)$ = maximum effective strength,

$\sigma_\phi(\varepsilon^P)$ = curvature parameter for strength surface,

$\varepsilon^P$ = plastic shear deformation.

[2] MINKLEY, W. (2004): Gebirgsmechanische Beschreibung von Entfestigung und Sprödbrucherscheinungen im Carnallitit.
Schriftenreihe des Institutes für Gebirgsmechanik- Band 1, Shaker Verlag Aachen

[3] MINKLEY, W.; MÜHLBAUER, J.; STORCH, G. (2007): Dynamic processes in salt rocks – a general approach for softening processes within the rock matrix and along bedding planes.
6th Conference on the Mechanical behaviour of Salt, SALTMECH6, Hannover, Juni 2007

Equation (2.2) can also be written as:

$$N_\phi = 1 + \frac{1}{\frac{1}{N_\phi^L - 1} + \frac{\sigma_3}{\sigma_{MAX} - \sigma_D}} \tag{2.4}$$

where $N_\Phi^L$ is the well-known friction angle relation of the linear MOHR-COULOMB failure criterion which does not depend on stresses. For $\sigma_3 = 0$, it follows that:

$$N_\phi = N_\phi^L = \frac{1+\sin\phi}{1-\sin\phi}. \tag{2.5}$$

The non-linear failure criterion contains only one additional parameter $\sigma_{MAX}$. The physical meaning of $\sigma_{MAX}$ becomes evident when plotting the failure criterion as $\sigma_1$ - $\sigma_3$ = f($\sigma_3$). Here, $\sigma_{MAX}$ is the maximum effective stress the rock can carry and to which the failure criterion moves towards with increasing minimum principal stress $\sigma_3$ (Fig. 2.1). For salt rocks under mining conditions the non-linearity of the failure envelope cannot be ignored.

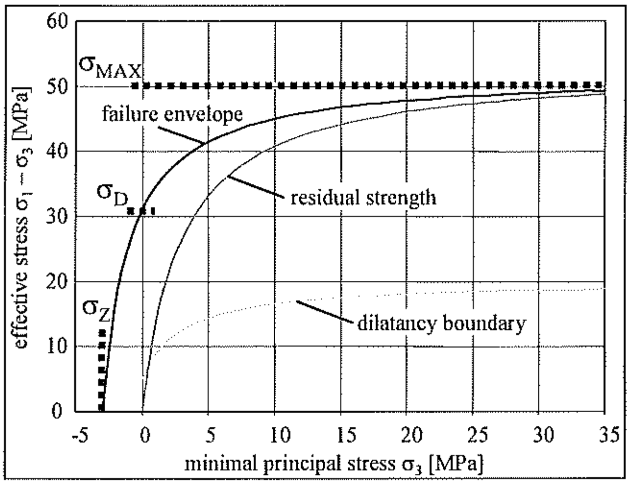


*Fig. 2.1: Yield points in the visco-elasto-plastic constitutive model.*

From equation (2.4) follows:

$$\sigma_{MAX} \to \infty: \qquad N_\phi = N_\phi^L,$$

i.e., under the assumption of an unlimited maximum effective strength, the modified non-linear MOHR-COULOMB model degenerates into the classical MOHR-COULOMB model. The non-linear failure criterion describes both compression as well as tension. More precisely, the tensile strength is given by:

$$\sigma_Z = \frac{1}{2}\cdot\left(\sigma_\phi + \sigma_{MAX}\right) - \sqrt{\frac{1}{4}\left(\sigma_\phi + \sigma_{MAX}\right)^2 - \sigma_D \cdot \sigma_\phi} \qquad (2.6)$$

Approximately is valid:

$$\sigma_Z \approx \frac{\sigma_D}{\sigma_{MAX}} \cdot \sigma_\phi \qquad (2.7)$$

The compressive strength $\sigma_D$, the tensile strength $\sigma_Z$, the maximum effective strength $\sigma_{MAX}$ and the curvature parameter $\sigma_\Phi$ are related by:

$$\sigma_\phi = \frac{\sigma_{MAX} - \sigma_Z}{\frac{\sigma_D}{\sigma_Z} - 1} \qquad (2.8)$$

$$\sigma_\phi = \frac{\sigma_{MAX} - \sigma_D}{N_\phi^L - 1} \qquad (2.9)$$

From the modified non-linear MOHR-COULOMB failure criterion (equation (2.3)), the flow rule for plastic flow can be deduced (pressure with negative sign):

$$f_S = \sigma_1 - \sigma_3 + \sigma_D - \frac{\sigma_{MAX} - \sigma_D}{\sigma_\phi - \sigma_3} \cdot \sigma_3 \qquad (2.10)$$

The plastic potential for non-associated flow is given by:

$$g_s = \sigma_1 - \sigma_3 - \frac{\sigma_{MAX,\psi} - \sigma_D}{\sigma_\psi - \sigma_3} \cdot \sigma_3 \qquad (2.11)$$

where $\sigma_{MAX,\psi}(\varepsilon^p)$ = maximum effective strength at the dilatancy boundary; and

$\sigma_\psi(\varepsilon^p)$ = curvature parameter of the dilatancy function.

If the failure envelope is reached, plastic deformations occur in addition to the elastic deformations. Using the flow rule, the plastic incremental deformation part can be determined:

$$\Delta\varepsilon_i^P = \lambda_S^* \cdot \frac{\partial g_s}{\partial \sigma_i} \qquad i = 1,2,3 \tag{2.12}$$

The determination of the multiplier $\lambda_S^*$ in Equation (2.12) is obtained for $f_S = 0$.

For volume increase (dilation) is valid:

$$\frac{\Delta V}{V_0} = \varepsilon_{VOL}^P = \left(N_\psi - 1\right) \cdot \varepsilon_1^P \tag{2.13}$$

with the dilation function $N_\psi$

$$N_\psi = 1 + \sigma_\psi \frac{\left(\sigma_{MAX,\psi} - \sigma_D\right)}{\left(\sigma_\psi - \sigma_3\right)^2} \tag{2.14}$$

For $\sigma_3 = 0$, it follows from equations (2.13) & (2.14):

$$\frac{\varepsilon_{VOL,0}^P}{\varepsilon_1^P} = \frac{\sigma_{MAX,\psi} - \sigma_D}{\sigma_\psi} \tag{2.15}$$

where

$$\frac{\varepsilon_{VOL,0}^P}{\varepsilon_1^P} = \tan\beta^0$$

is the slope of the volume deformation curve $\varepsilon_{VOL}^P = f\left(\varepsilon_1^P\right)$ in the dilation area under uniaxial load ($\sigma_3 = 0$). Therefore, the dilation function can be written as:

$$N_\psi = 1 + \frac{\sigma_\psi^2}{\left(\sigma_\psi - \sigma_3\right)^2} \cdot \tan\beta^0 \tag{2.16}$$

where $\tan(\beta^0)$ and $\sigma_\psi$ depend on the plastic deformation $\varepsilon_1^P$.

If the curvature parameter of the dilatancy function moves in such a way that $\sigma_\psi \to \infty$, a linear relation yields:

$$N_{\psi}^{L} = 1 + \tan\beta \qquad (2.17)$$

with the common description of the dilation with a constant stress-independent dilation angle

$$\psi = \arcsin\left(\frac{\tan\beta}{2+\tan\beta}\right). \qquad (2.18)$$

The elastic constants (shear modulus G and in analogy the bulk modulus K) are given by an empirical relation:

$$G = G_R + \frac{1}{1 + f \cdot \varepsilon_{VOL}^{p}} \cdot G_0 \qquad (2.19)$$

where $G_0 = G_I - G_R$ with $G_I$ = shear modulus of intact rock, $G_R$ = shear modulus of rock in the post-failure region and f = material parameter.

Besides the elasto-plastic characteristic, most salt rocks show viscous behavior. Therefore, the elasto-plastic softening model is combined with the BURGERS creep model (Fig. 2.2). The incremental form of the BURGERS model is given in the FLAC manuals (ITASCA, 2005[1]).

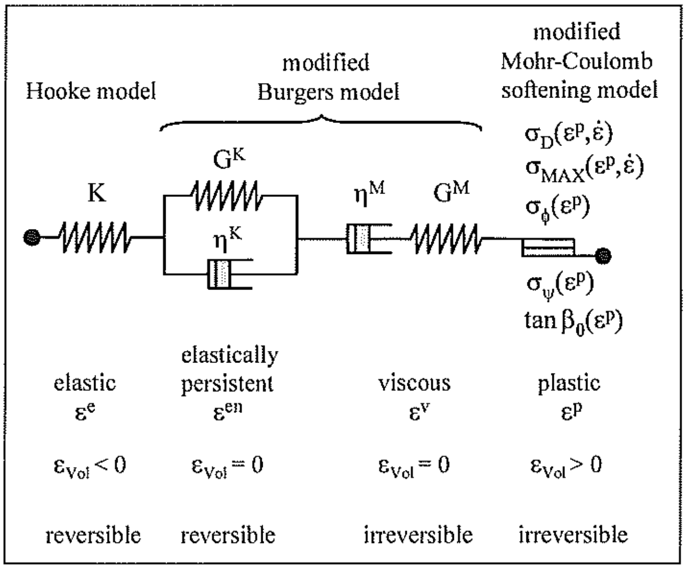


*Fig. 2.2: . Visco-elasto-plastic model concept.*

The model allows describing the creep behavior including creep rupture. The primary creep phase is modeled by the KELVIN-Model with KELVIN shear modulus $G^K$ and KELVIN viscosity $\eta_K$. The secondary creep phase is controlled by the MAXWELL viscosity $\eta_M$. The tertiary creep phase is governed by a dilation softening mechanism.

Within the visco-elasto-plastic material model, the stress dependence of the creep rate is governed by the exponential dependence of the MAXWELL viscosity $\eta^M$ on the deviatoric stress $\sigma_V$:

$$\eta^M = \eta_0^M \cdot e^{m \cdot \sigma_V} \quad (2.20)$$

## 2.4 Evaluation criteria

The evaluation of stability, consistency and geological tightness of NaCl-brine-production caverns is performed by means of criteria which have been elaborated on the basis of long-standing experience obtained in assessing the hydro-geologic dangers and operational reliability of hydrologic protective layers in salt rock mining in Central Germany as well as in dimensioning caverns for underground storage projects.

Minimum stress or fracturing criterion for brine-production caverns:

This criterion requires that the minimum stress induced by the rock pressure, $\sigma_{MIN} = \sigma_3$, must always be higher or equal than the internal pressure $p_i$ prevailing in the cavern to prevent fractures within or penetrations through the salt barrier:

$$n_{FRAC} = \frac{\sigma_{MIN}}{p_i} \geq 1 \quad (2.21)$$

Utilization of the stability $\eta$ of the solid rock massif

For ensuring the stability of the cavity system during leaching operation the utilization of short-term stability of the surrounding support elements (pillars, cavity contour, and roof pillar) is of decisive importance. The utilization degree $\eta$ has been defined as follows:

$$\eta = \frac{\sigma_{eff}}{(\sigma_{eff})_{MAX}} \quad (2.22)$$

where $\sigma_{eff}$ designates the effective stress acting within the rock element (and evidenced by calculations) and $(\sigma_{eff})_{MAX}$ designates the effective rupture stress as derived from triaxial short-time compression tests as a function of the effective minimum pressure constraint $\sigma_{MIN}$. For a long-term stable operation the utilization degree of the short-term strength $\eta$ should not exceed the following values:

Contour: $\eta \leq 40$ %

Support elements (roof pillar, pillar): $\eta \leq 25$ %.

## 3. Generic rock mechanical model "NaCl-brine-production cavern Haaksbergen"

The generic rock mechanical model (annex 2) comprises a sector of the deposit in the depth of 500 m to 1100 m. The model is a rotational-symmetric model where the right hand model boundary (radius: 158 m) acts as the symmetry surface between the investigated cavern and the neighbouring caverns within the cavern field, which is horizontally fixed. The left hand boundary of the model is the rotational axis and is also fixed horizontally. The basis of the model is located within the Upper Carboniferous. It is 150 m below the leaching level and is vertically fixed. The top of the model (Lower Buntsandstein) is normally loaded with 12.4 MPa, which corresponds to the average weight of the overlying overburden (average lithostatic depth pressure gradient $\gamma$ = 24.8 kPa/m). The model comprises a total of 10653 elements and represents the layers of the deposit (annex 1) as shown in Tab. 3.1:

Table 3.1: Depth and occurring rock formations

| Depth [ m ] | Rock formation |
|---|---|
| 500 – 540 | Lower Buntsandstein |
| 540 – 680 | z3 Salt<br>z3 Main Anhydrite<br>z3 Grey Salt Clay<br>z2 Salt<br>z2 Basal Anhydrite<br>z2 Carbonate<br>z1 Upper Anhydrite |
| 680 – 950 | z1 Salt (Werra Steinsalz ) |
| 950 – 1000 | z1 Lower Anhydrite |
| 1735 – 1745 | Grauer Salzton |
| 1000 – 1100 | Upper Carboniferous |

The cavern cavity is modelled in depths of 750 – 915 m (annex 1). The lower part of the cavern in the depth of 885 m to 915 m has the shape of a half rotational-ellipsoid. The medium part (cavern equator) is a cylinder with a diameter of 135 m. The domed cavern roof was modelled in the shape of a rotational-paraboloid.

The cavern sump which (among others) consists of hardly soluble and insoluble residuals (e.g. anhydrite, clay), recristalised rock salt, quarry rock salt and brine has generally a volume of about 5 - 20 % of the whole leaching volume. Mechanical properties like undrained hydraulic backfill could be assigned to the sump. However, since there are no material investigations, the cavern sump is assigned to the cavern cavity during the numerical calculations. This results in an over-all volume of the generic cavern model of 1.673 million $m^3$.
Assuming that the in-situ-utilisation of the generic cavern model is 85 % the leaching volume is 1.42 million $m^3$ which results in a salt production capacity of about 2.43 million tons.

Constitutive models and material parameters have been assigned to the modelled layers according to their respective mechanical properties and specific behaviour. Basis for this are parameter sets which were available at the IfG Leipzig from several comparable deposits in Central Germany.

The description of the plastic material behaviour of the non salt layers has been carried out using the linear elasto-plastic MOHR-COULOMB model specially implemented in the FLAC code.

The MOHR-COULOMB failure criterion is as follows:

$$(\sigma_1)_B = \sigma_3 \cdot N_\Phi + 2 \cdot C \cdot \sqrt{N_\Phi} \qquad \text{mit } N_\Phi = \frac{1+\sin\Phi}{1-\sin\Phi}.$$

Here, C is the cohesion and $\phi$ the angle of friction.

The strength and deformation parameters ($\dot{\varepsilon}$ in 1/h; t in h; $\sigma$ in MPa) which have been used for the rock salt as basis for the visco-elasto-plastic softening model are summarized in Tables 3.2 to 3.4.

*Table 3.2: Dilatancy parameters for rock salt*

| $\varepsilon^p$ [ % ] | 0.0 | 0.2 | 1.0 | 2.0 | 5.0 |
|---|---|---|---|---|---|
| **$\tan\beta_0$ [ - ]** | 0.0 | 1.50 | 2.20 | 2.95 | 4.0 |
| **$\sigma_\psi$ [ MPa ]** | 0.2 | 2.0 | 1.2 | 1.1 | 1.0 |

*Table 3.3: Strength parameters for rock salt*

| **Plastic shear strain $\varepsilon^p$ [%]** | **Compressive strength $\sigma_D$ [MPa]** | **Maximum effective strength $\sigma_{MAX}$ [MPa]** | **Curvation parameter $\sigma_\phi$ [MPa]** |
|---|---|---|---|
| 0 | 4.0 | 31.2 | 1.1 |
| 1,0 | 16.8 | 33.6 | 2.2 |
| 2,0 | 20.4 | 36.0 | 3.0 |
| 3,0 | 22.0 | 36.4 | 3.0 |
| 7,0 | 24.3 | 43.6 | 3.8 |
| 10,0 | 19.2 | 37.2 | 0.6 |
| 13,0 | 0 | 46.4 | 0.8 |
| 15,0 | 0 | 92.0 | 5.0 |

*Table 3.4: Creep parameters for rock salt*

| Rock material | Kelvin body | | Maxwell body | | |
|---|---|---|---|---|---|
| | $G^K$ [MPa] | $\eta^K$ [MPa·d] | $G^M$ [GPa] | $\eta^M$ [MPa·d] | m [$MPa^{-1}$] |
| Rock salt | $6.3*10^4$ | $1.7*10^5$ | $1.0*10^4$ | $10^7$ | 0.3 |

Table 3.5 summarizes the stability parameters for the non salt layers which have been used during the numerical analysis.

*Table 3.5: Stability parameters of the non salt layers*

| **Rock formation** | **Material – model** | **$\Phi$ [ ° ]** | **C [ MPa ]** |
|---|---|---|---|
| Overburden | MOHR - COULOMB | 45 | 5 |
| Under laying basement | MOHR - COULOMB | 45 | 5 |

Between the layers capable of creep and the layers non-capable of creep interfaces have been modelled. These behave like bedding planes and planes of separation respectively, on which a horizontal sliding or a vertical opening of the interfaces can occur if the failure criterion is violated ($k_n$ = 10 GPa, $k_s$ = 1 GPa, $\Phi$ = 15°, C = 1 MPa).

The primary stress state of the rock mass is calculated from the densities $\rho$ determined for the individual layers (Annex 1), the acting factors of lateral pressure $\lambda$ (ratio between horizontal and vertical stress) and the weight of the overburden on top of the model. For most of the regions in Central Europe it can be assumed that the vertical stress component is equal to the lithostatic pressure of the overlying overburden and can be calculated as follows:

$$\sigma_V = g \cdot \sum_i \rho_i \cdot \Delta H_i \,,$$

where g is the gravitational constant, $\rho_i$ is the mean density and $\Delta H_i$ is the height of the individual overlying rock layers.

The creep and relaxation abilities of the considered rocks have a great influence on the development of the horizontal primary stress component. In rock layers with pronounced creep and relaxation behaviour, like salts and partly clay stones, measurement results (GROß, MINKLEY & PENZEL (1986)[4]; NATAU, LEMPP & BORM, 1986[5]) confirm the creation of an isotropic stress state with equal pressure in all directions, which corresponds to the lithostatic depth pressure of the overburden $\sigma_H \approx \sigma_h \approx \sigma_V$. Therefore the factor of lateral pressure $\lambda$ inside these layers is assumed as follows:

$$\lambda \approx \lambda_H = \frac{\sigma_H}{\sigma_V} \approx \lambda_h = \frac{\sigma_h}{\sigma_V} \approx 1.$$

However, in layers with extremely low ductility (e.g. anhydrite, carbonate etc.) the differences between horizontal and vertical stress will in general not be balanced even within geological timespans. However, one has to assume a considerably increased horizontal stress component also for these layers in the primary stress state compared to the assumption of a purely elastic state, for which $\sigma_H = \sigma_h = \lambda \cdot \sigma_V$ with $\lambda = \frac{\nu}{1-\nu}$ would hold. This assumption has in principle been verified by numerical calculations at IfG as well as by in-situ measurements in

[4] GROß, U.; MINKLEY, W.; & PENZEL, M. (1986): Ergebnisse zur Untersuchung von Gebirgsspannungszuständen und ihre Anwendung für die Hohlraum- und Ausbaudimensionierung. Proc. Int. Symposium on Rock Stress and Rock Stress Measurements, Stockholm, 531-536.

[5] NATAU, O.; LEMPP, CH.; BORM, G. (1986): Stress relaxation monitoring prestressed hard inclusions. . Proc. Int. Symposium on Rock Stress and Rock Stress Measurements, Stockholm, 509-513.

anhydrite layers, where λ-values of 0.7 to 1.0 were obtained (LEMPP, CH. & RÖCKEL, TH., 1999[6]).

Because the distribution of the horizontal primary stress state inside the considered deposit is not known, a factor of lateral pressure of $\lambda = 0.7$ is assumed during the first stage of the numerical calculations to determine the stability and impermeability analysis of a generic NaCl-brine-production cavern at Haaksbergen.

Annex 3 summarizes the values of ρ and λ which were used in the first stage of calculation. According to these specifications an isotropic stress state between 17.2 MPa (H = 680 m) and 22.6 MPa (H = 950 m) results inside the Werra Steinsalz (z1WS) rock salt. Inside the layers reacting elasto-plastically (overburden, underlying basement) the horizontal pressure is reduced by 8 to 4 MPa compared to the vertical stress because of the assumed value of $\lambda = 0.7$.

The simulation of the cavern leaching process has been done in one stage by removing the elements which correspond to the cavern area and by loading the resulting contour with a pressure equal to the difference between primary stresses and pressures calculated from the weight of the brine column filling the well from the surface to the cavern ($p_i = \gamma_S \cdot H$ , $\gamma_S$ = 11.8 kPa/m). Thus the pressure inside the cavern is 8.8 MPa at the roof and 10.8 MPa at the floor ($p_{wellhead} = 0$).

## 4. Results of rock mechanical modelling

Fig. 4 to 6 summarize the results of the stress-deformation-analysis concerning the intended brine production caverns at Haaksbergen.

Considering the forecasted stress states which occur during the simulated leaching process, it can be deduced that the minor principle stress inside the rock salt is always greater than the brine pressure (Fig. 4; left). Even in case a wellhead pressure of 5 MPa is applied (as to reduce volume convergence) the minor principle stress is always greater than the resulting cavern pressure (Fig. 4; right). Thus the geological impermeability of the deposit and of the overlying and underlying rock mass can be guaranteed.

[6] LEMPP, CH. & RÖCKEL, TH. (1999): Das Spannungsfeld in der weiteren Region nördlich des Harzes. Martin-Luther-Universität Halle-Wittenberg

Considering the resulting stress at the cavern contour and its stability (Fig. 5), it can be concluded that the degree of utilisation of the strength (determined by short-term strength tests) increases up to 22 % in maximum. For the roof pillar and the centre of the pillar between caverns degrees of utilisation of less than 10 % have been determined. These degrees of utilisation are valid for the leaching process. Due to the stress relaxation induced by creep deformation the degrees of utilisation are reduced in the course of further time under brine pressure. The degree of utilisation of the strength can be further reduced by applying an additional wellhead pressure.

Generally, it can be concluded that the numerical calculations show a rock mechanically stable and safe state during the whole leaching process and for the subsequent period where it is assumed that the cavern pressure stays at least at brine pressure.

The volume convergences which were forecasted with the help of the developed numerical model are shown in Fig. 6. In the phase of the leaching process, which was carried out in the numerical model over a period of 2 years a volume convergence of totally 0.48 % had been predicted. In the stationary case the calculated rate of volume convergence is 2 ‰/a.
In the case of applying a wellhead pressure of 5 MPa the rate of volume convergence is reduced to 0.4 ‰/a.

## 5. Summary and Conclusions

For the Haaksbergen brine production field a generic rock mechanical model has been developed with the following layout parameters:

- Minimum thickness of z1 salt roof: 70 m
- Maximum cavern diameter: 135 m
- Cavern spacing 300 m
- Minimum salt pillar between caverns: 165 m
- Domed shape of the cavern roof
- Average salt production per cavern: 2.4 Mio. t.

Because no location specific material parameters were known so far, material parameters were adopted from a comparable deposit nearby that have been determined by IfG Leipzig within the scope of different projects. This has been assumed for rock salt, overburden and underlying basement lithologies.

Based on the performed geomechanical calculations it can be recapitulatory evaluated that:

- The stability and impermeability of the salt rock mass surrounding the investigated brine-production cavern is guaranteed.
- The volume convergence rate is about 2 ‰/a ($p_{wellhead}$ = 0) or 0.4 ‰/a ($p_{wellhead}$ = 5 MPa) in the stationary state.

It has to be mentioned that the simulation of the cavern leaching in a single step (i. e. not by a continuous process over a period of 2 years) leads to an overestimation of the volume convergence rate.

On order to reduce the volume convergence and thus the surface subsidence it is recommended:

- to limit the number of caverns that will be leached at the same time and
- to minimise the stand-by operation period before cavern abandonment.

**List of Figures and Annexes**

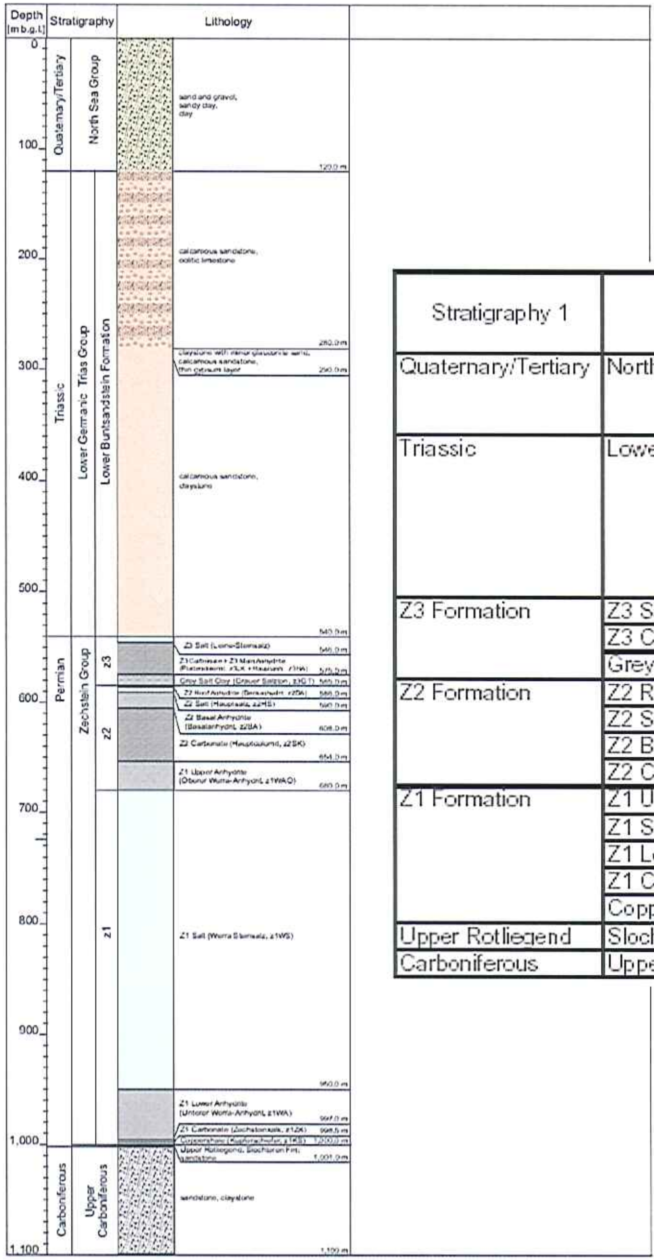


| Stratigraphy 1 | Stratigraphy 2 | Depth from [m TVD] | Depth to [m TVD] | TVD-Thickness | Haaksbergen area Lithology | Haaksbergen area rock density (bulk) [g/cm³] |
|---|---|---|---|---|---|---|
| Quaternary/Tertiary | North Sea Group | 0.0 | 20.0 | 20.0 | sand and gravel | 2.00 |
| | | 20.0 | 40.0 | 20.0 | sandy clay | 2.00 |
| | | 40.0 | 120.0 | 80.0 | clay | 2.30 |
| Triassic | Lower Germanic Trias Group | 120.0 | 280.0 | 160.0 | calcareous sandstone, oolitic limestone | 2.60 |
| | | 280.0 | 290.0 | 10.0 | claystone with minor glauconite sand, calcareous sandstone, thin gypsum layers | 2.65 |
| | | 290.0 | 540.0 | 250.0 | calcareous sandstone, claystone, rare gypsum/anhydrite veins | 2.65 |
| Z3 Formation | Z3 Salt | 540.0 | 546.0 | 6.0 | rock salt | 2.17 |
| | Z3 Carbonate + Z3 Main Anhydrite | 546.0 | 575.0 | 29.0 | limestone, anhydrite | 2.62 |
| | Grey Salt Clay | 575.0 | 585.0 | 10.0 | clay | 2.30 |
| Z2 Formation | Z2 Roof Anhydrite | 585.0 | 586.0 | 1.0 | anhydrite | 2.88 |
| | Z2 Salt | 586.0 | 590.0 | 4.0 | rock salt | 2.17 |
| | Z2 Basal Anhydrite | 590.0 | 608.0 | 18.0 | anhydrite | 2.91 |
| | Z2 Carbonate | 608.0 | 654.0 | 46.0 | dolomitic limestone | 2.85 |
| Z1 Formation | Z1 Upper Anhydrite | 654.0 | 680.0 | 26.0 | anhydrite | 2.92 |
| | Z1 Salt | 680.0 | 950.0 | 270.0 | rock salt | 2.08 |
| | Z1 Lower Anhydrite | 950.0 | 997.0 | 47.0 | anhydrite | 2.92 |
| | Z1 Carbonate | 997.0 | 998.5 | 1.5 | dolomite | 2.70 |
| | Coppershale | 998.5 | 1.000.0 | 1.5 | organic rich claystone | 2.80 |
| Upper Rotliegend | Slochteren Formation | 1.000.0 | 1.001.0 | 1.0 | sandstone | 2.60 |
| Carboniferous | Upper Carboniferous | 1.001.0 | 1.100.0 | 99.0 | sandstone, claystone | 2.60 |

Akzo Nobel - XLT Planning Hengelo
Haaksbergen area - Lithology and related rock densities

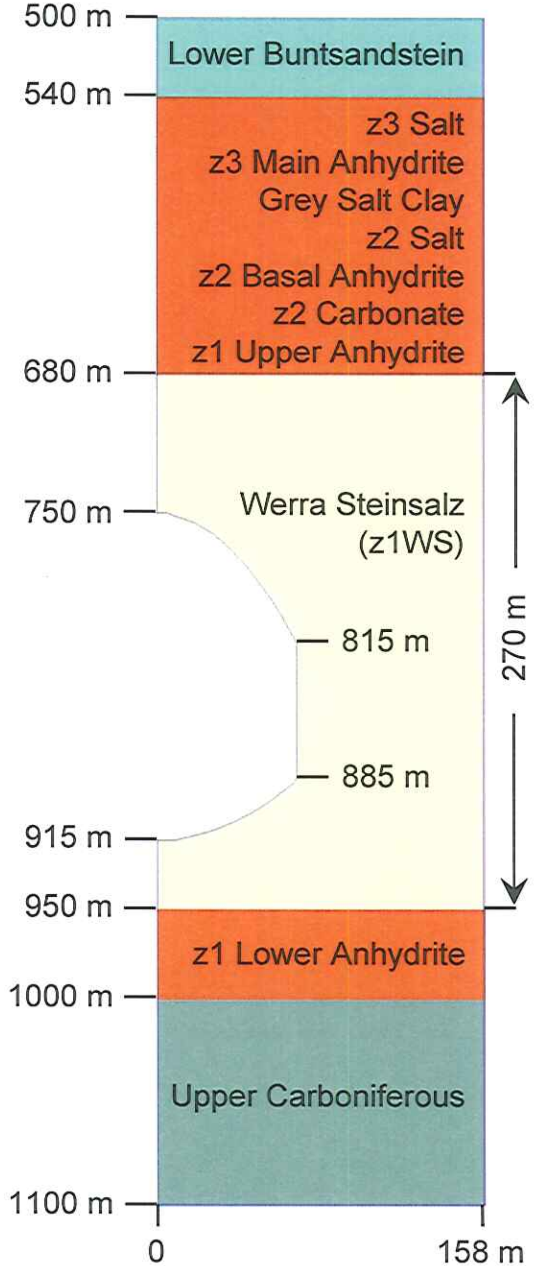


Rock mechanical scale:

Depth: 750 m – 915 m (h = 165 m)

Radius: R = 67.5 m ($A_{MAX}$ = 14 300 $m^2$)

Volume: $V_{MAX}$ = 1.673 Mio. $m^3$

utilisation in situ: 85 %

$V_{Sol}$ = 1.422 Mio. $m^3$

$V_{Hohl} \approx 0{,}9 \cdot V_{Sol}$ = 1.280 Mio. $m^3$

→2.43 Mio. t Salt production capacity

Cavern spacing

a = 300 m

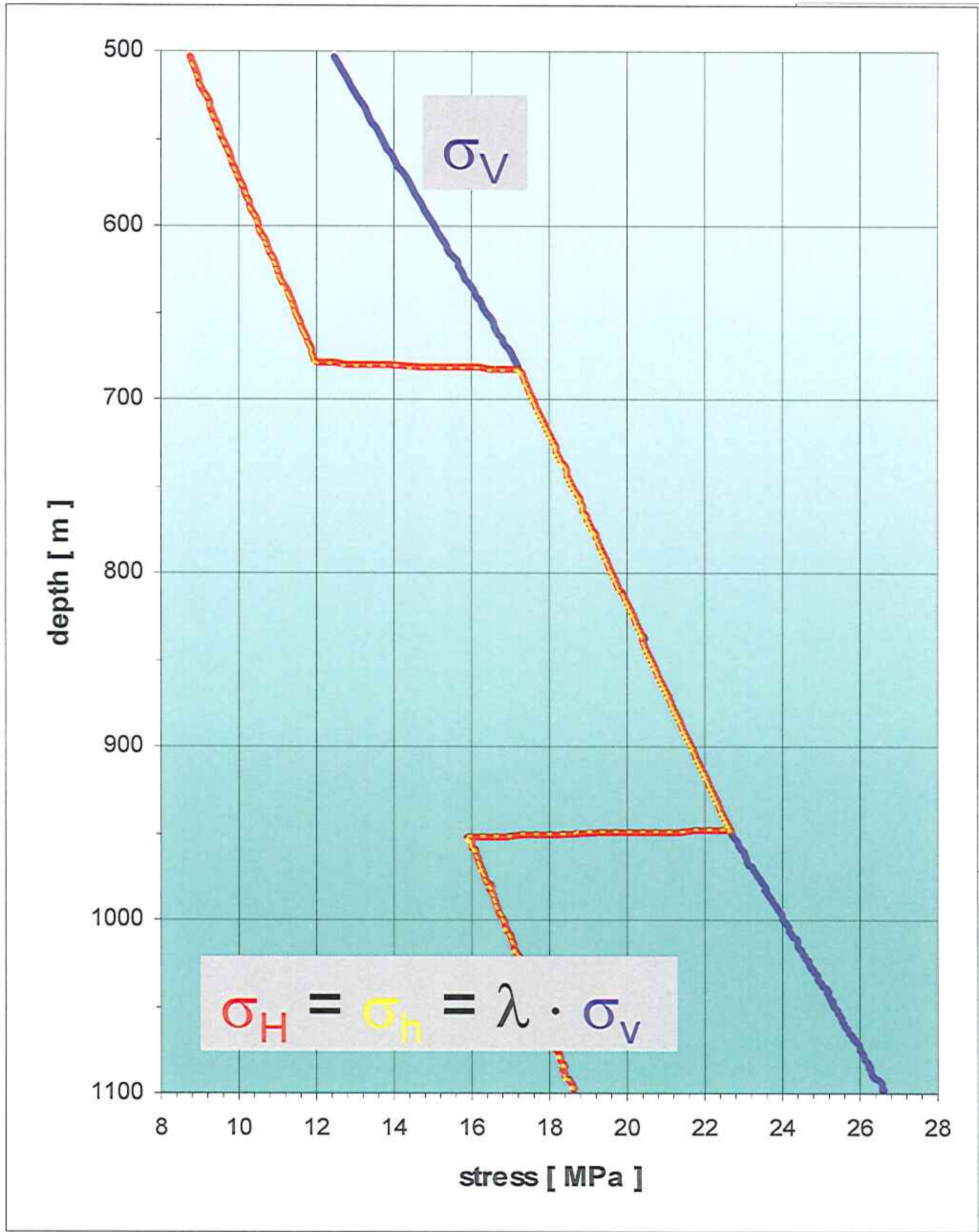


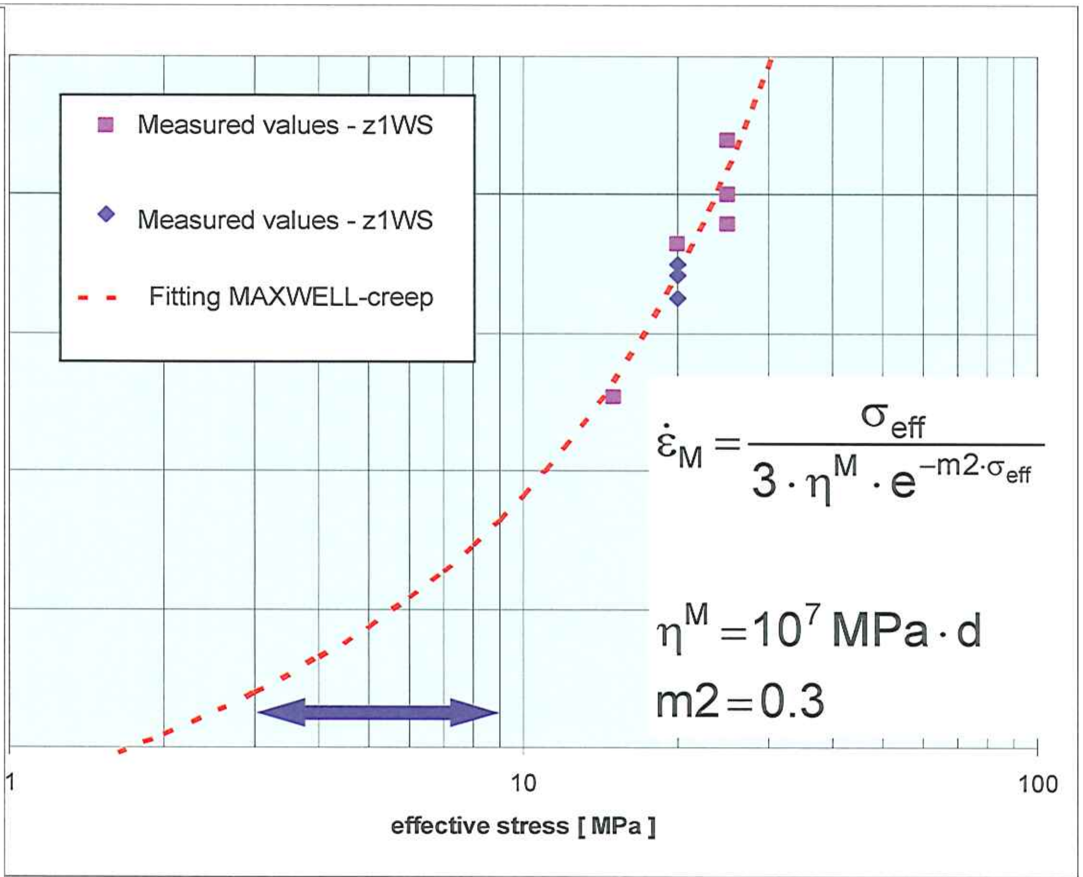


| Strata | $\bar{\gamma}$ [ kPa/m ] | λ [ – ] |
|---|---|---|
| Overburden | 26.667 | 0.7 |
| Rock salt | 20.407 | 1.0 |
| Under laying basement | 26.467 | 0.7 |

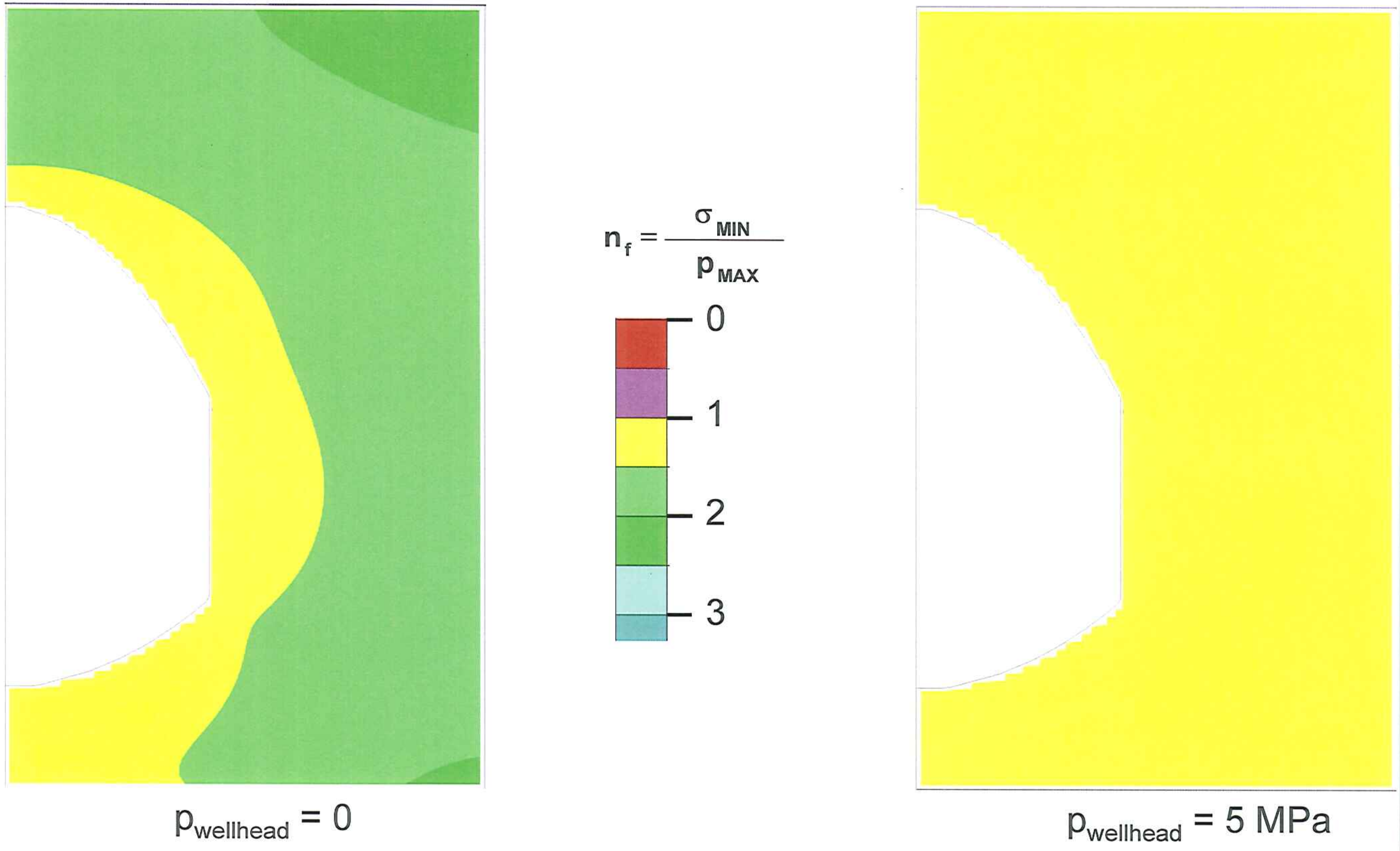
$n_f = \frac{\sigma_{MIN}}{p_{MAX}}$
0
1
2
3
$p_{wellhead} = 0$
$p_{wellhead} = 5$ MPa

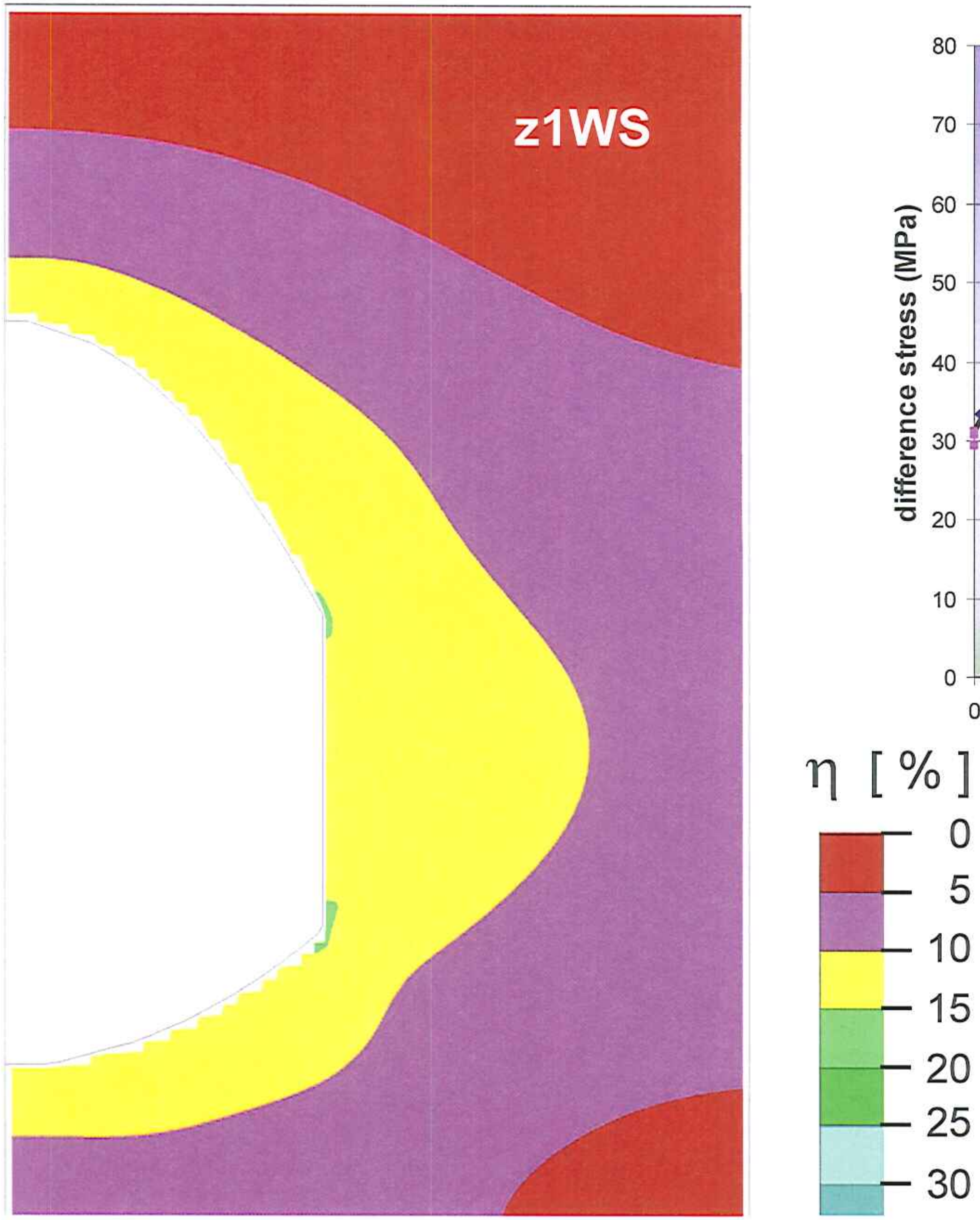


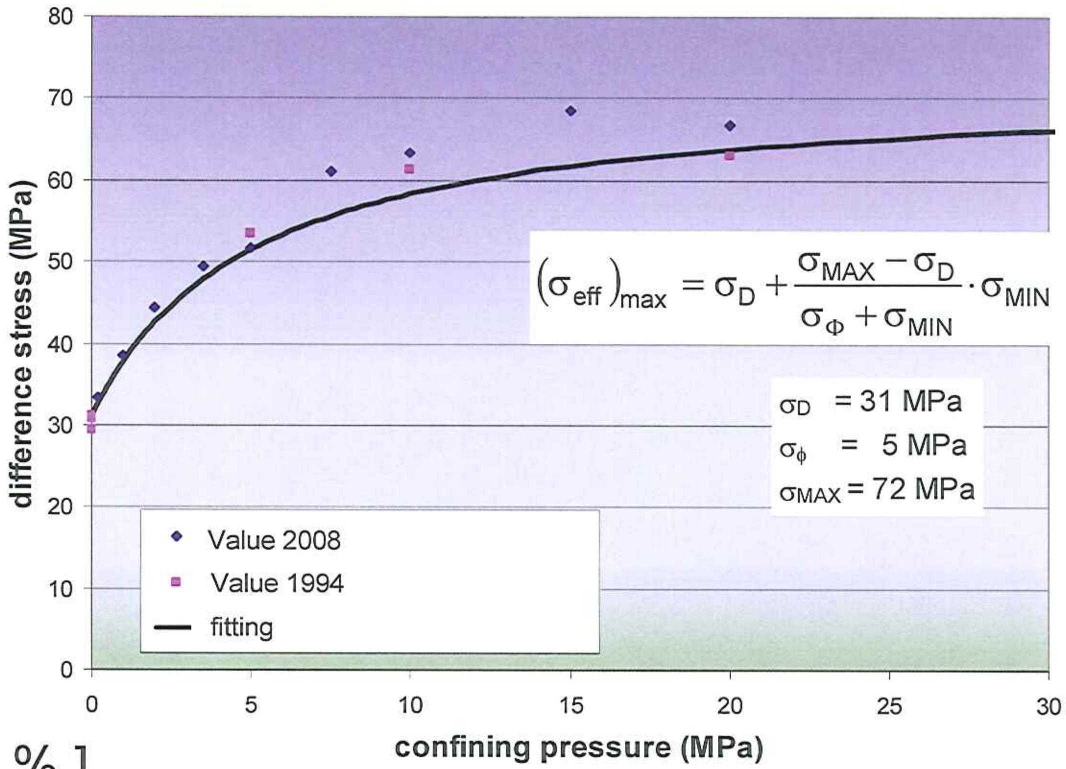


$$\eta = \frac{\sigma_{eff}}{(\sigma_{eff})_{MAX}}$$



Strength of z1WS and degree of utilisation η

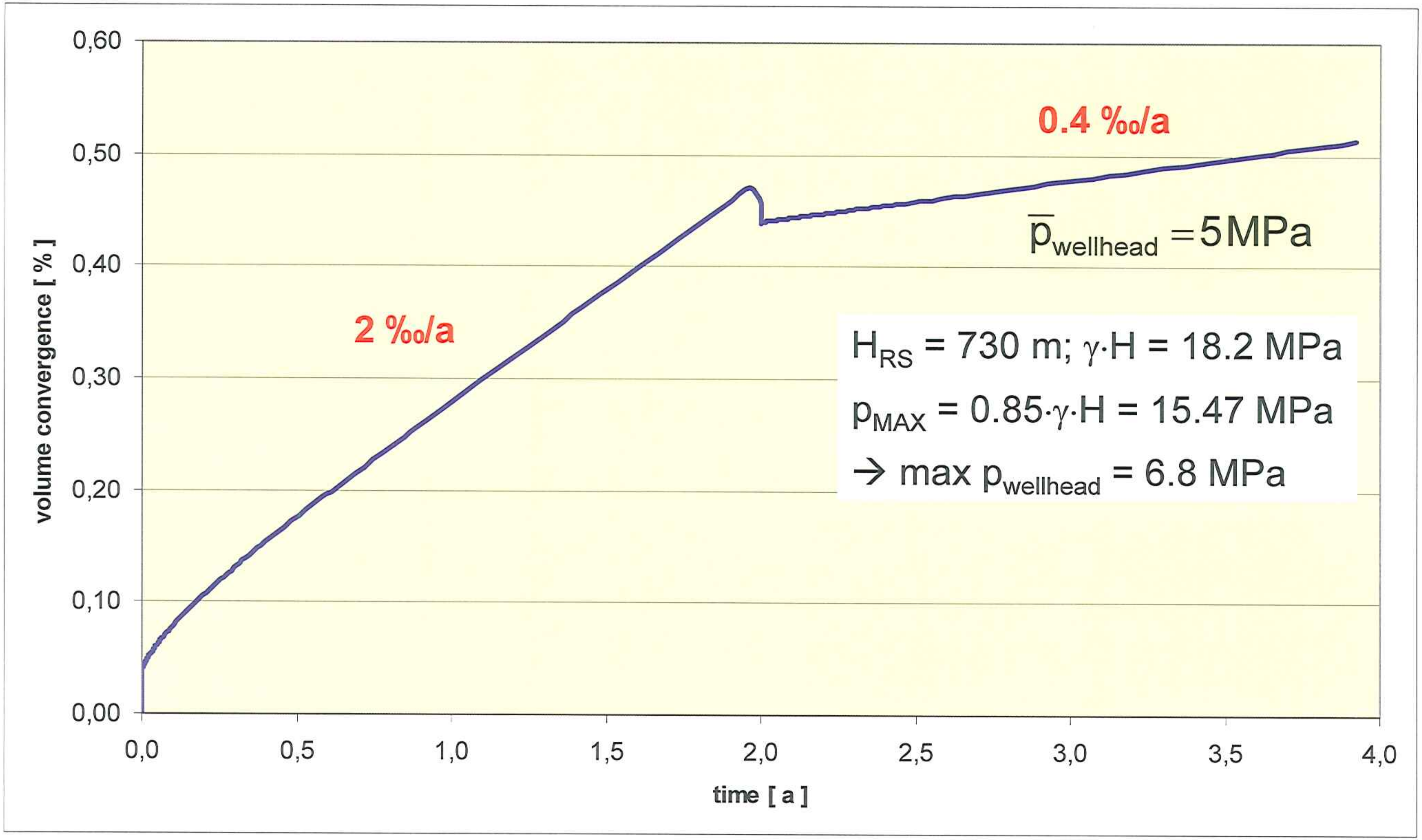


Institut für Gebirgsmechanik GmbH
Research · Testing · Consulting · Expertise

Calculated volume convergence

Annex 6